Data Modelling of Physical-Mechanical Processes in Nano Concrete with the Ensemble of Pores

Roman Mysiuk [1], **Iryna Mysiuk** [1], **Grzegorz Pawlowski** [2]

[1] *Ivan Franko National University of Lviv*
1 Universytetska Street, Lviv, Ukraine, 79000

[2] *Zaklad Handlowo-Uslugowy BHP*
17 Kostrzynska Street, Gorzyca, Poland, 69-113

DOI: 10.22178/pos.85-6

JEL Classification: L74, L86

Received 20.08.2022
Accepted 20.09.2022
Published online 30.09.2022

Corresponding Author:
Roman Mysiuk
mysyukr1@ukr.net

Abstract. This paper assesses the strength of nano concrete and methods of strengthening it by adding nanoparticles. Since concrete structures are exposed to the environment and external influences, there is a need to enhance resistance to destruction. Modelling of behaviour and the nature of changes in indicators of chemical shrinkage and destructive load is performed. Data analysis is executed based on the data of ordinary portland cement pastes and cement-fly ash pastes. The results are compared with admixtures to these materials of three nanomaterials: nanolimestone, nanosilica, and nanoclay. The percentage ratio for compressive strength for materials is established. The data processing and visualization of the results are presented using an interactive web page using dynamic mathematical calculations of approximation and interpolation based on the entered data. The data is processed using modern open-source libraries and stored in the database. The work aims to develop a methodological approach for modelling physico-mechanical processes in nano concrete, considering nanoparticles and an ensemble of pores.

Keywords: nanomaterial; compressive strength; computer modelling.

INTRODUCTION

One of the primary materials in construction is concrete based on sand-cement mixtures. This material must withstand heavy loads and be stable under various weather conditions, so the compressive strength parameter can be considered an additional factor in improving the stability of concrete structures [1, 2].

Forecasting the strength and durability of nano concrete is expedient to assess the levels of reliability and resource using optimisation methods. Fundamental processes in this context relate to mechanical loads and the pore medium. It is possible to simulate the penetration of the pore fluid into the solid-phase frame and the redistribution (filtration) of the fluid in the pore space of the material. The porous medium is characterised by integral parameters, such as the volume of the pore space, porosity and permeability [3, 4, 5]. The liquid (water) in the porous medium of nano concrete is considered implicitly and is also characterised by integral parameters: mass, density, pressure, and dynamic viscosity [3, 4].

The work aims to model such physical and mechanical processes as compressive strength, water and calcium hydroxide content in nano concrete, considering nanoparticles and the ensemble of pores.

One of the tasks of this work is the development of a strength criterion for nano concrete, taking into account the ensemble of pores based on the approaches of surface physics and fracture mechanics. In addition, the evaluation of the quality of nano concrete, taking into account the physical and mechanical characteristics of the rigid frame and porous medium, is taken into account.

Another task is the formulation of criterion ratios based on evaluating the strength, reliability,

strengthening parameter and residual resource of nano concrete, and taking into account the porous medium.

MATERIAL AND METHODS

The non-associated law of plastic flow with the Mises-Schleicher criterion is used to describe stress relaxation and accumulation of inelastic deformation in nano concrete, which is used to model the behaviour of brittle natural and artificial materials [5, 6]:

$$Y = \alpha\sigma_{s(eff)} + \sigma_{\text{int}} / \sqrt{3} = \alpha\left(\sigma_s + P_{pr}\right) + \sigma_{\text{int}} / \sqrt{3}, \quad (1)$$

where Y – adhesion characteristic (elastic limit of the material in pure shear); σ_{int} – stress intensity; α – coefficient of internal friction; $\sigma_{s(eff)}$ – average effective stress; P_{pr} – actual pressure value in the pore medium of the element.

The main defining relations connecting the averaged stresses and deformations of the solid-phase frame of the element, as well as the fluid pressure in the pore (capillary) space of the element, are of the form [5, 6]:

$$\Delta\sigma_{\alpha\beta} = 2G(\Delta\varepsilon_{\alpha\beta} - \delta_{\alpha\beta}a\Delta P_{pr} / K) + \delta_{\alpha\beta}(1 - 2G / K)\Delta\sigma_s,$$

$$\delta V = \delta\varphi = \frac{a}{K}\Delta\sigma_s + \left(\frac{1}{K} - \frac{1+\varphi}{K_s}\right)\Delta P_{pr}, \quad (2)$$

$$\delta P_{pr} = K_L\left(\frac{\rho_L}{\rho_{L0}} - 1\right) = K_L\left(\frac{m_L}{\rho_{L0}V_p} - 1\right), \quad (3)$$

where $\delta\varphi=\varphi-\varphi_0$; $\delta V=(V_p - V_{p0})/V$; $\varphi=V_p/V$; $\varphi_0=V_{p0}/V$; σ_s – average tension; φ, φ_0 – current and initial value of porosity; Δ – the symbol of the increase of the corresponding variable per time step during the integration scheme of the equations of motion of the element of the continuous medium of nano concrete; $\varepsilon_{\alpha\beta}$, $\sigma_{\alpha\beta}$ – components of tensors of averaged strains and stresses in the volume element; G and K – shear modulus and all-round compression modulus of the element material in the absence of pore fluid (mixture); $\delta_{\alpha\beta}$ – Kronecker symbols; $a = (1 - K/K_s)$ – coefficient of porosity in the Biot model [6, 7]; K_s – module of comprehensive compression of the material of the frame walls.

V_p, V_{p0} – current and initial volume (in the undeformed element); V is the volume of the component; ρ_{L0}, P_{pr0}, – the equilibrium value of the density and pressure of the liquid under atmospheric conditions (in the absence of a mechanical limitation of the volume of the liquid); ρ_L – current density value in the pore medium of the element; K_L – modulus of comprehensive liquid compression (mixtures).

As a criterion for the destruction of the frame and cement mixture, the Drucker-Prager criterion is used, which derives the expression for the effective Tercaghi stresses [5, 8, 9]:

$$\sigma_f = 1,5(\beta - 1)\sigma_{s(eff)} + 0,5(\beta + 1)\sigma_{\text{int}} = \sigma_c, \quad (4)$$

where $\beta = \sigma_c/\sigma_t$; σ_c and σ_t – the value of the compressive and tensile strength of the frame material. For nonporous basalt, the traditional formulation of the Drucker-Prager criterion is used, in which instead of $\sigma_{s(eff)}$ (4) is used σ_s [5, 8, 9].

The Griffiths-Irwin-Orovan strength criterion is also used [10]:

$$\sigma_* = \sqrt{\frac{4E \cdot WPL}{\pi \cdot L_T(1 - \nu^2)}}, \quad (5)$$

where σ_* – compressive strength; L_T – pore diameter; WPL – specific energy spent on plastic deformation of the near-surface (interfacial) layer of the body, provided that a new (juvenile) surface is formed in it; E, ν – Young's modulus and Poisson's ratio of the frame, respectively.

In reinforced concrete, rust forms on the surface of the reinforcement. Corrosion products (in particular, rust) penetrate the pores. Parameter WPL is included in the expression I_a corrosion current [11]:

$$I_a = I_{as}(1 + \beta_w \cdot WPL) = \chi \cdot \Delta\psi_{ak}(1 + \beta_w \cdot WPL) / r, \quad (6)$$

where χ – electrical conductivity of the electrolyte; $\Delta\psi_{ak}$ – ohmic potential change between the anodic and cathodic parts (anode – top, cathode – edges of the crack (pores)); r – pore radius; I_{as}, β_w – constants that are determined from the experiment.

Ratios (1)–(6) and the quality criterion [11] will be used to estimate the parameters of the stress-strained state and the conditions for strengthening nano concrete.

The reliability parameter β_R (reliability) (security characteristic) based on the probabilistic approach is determined by the ratio [11]:

$$\beta_R = Y_{RM} / Y_{SRM}, \quad (7)$$

where Y_{RM} – strength reserve; Y_{SRM} – strength reserve standard.

There is a transitional state between the rigid frame and the pore. The energy of adhesive bonds γ_{ad} and its change $\Delta\gamma_{ad}$ depend on the energy characteristics of the frame and the pore medium. Formulate the interphase ratio of the strength criterion between the frame and the pore medium similar to the coating, taking into account the results of the article [12, 13, 14, 15]:

$$\delta\sigma_m \le \delta\sigma_{m*}, \delta\gamma_m \le \delta\gamma_{m*}, \delta A_{ad} \le \delta A_{ad*},$$
$$\delta\gamma_{vad} \le \delta\gamma_{ad*}, \quad (8)$$

where $\delta\sigma_m$ – change in interfacial tension; $\delta\gamma_m$ – change of interfacial energy; δ – the symbol of deviation (change) of the parameter or energy characteristic of the interfacial layer; δA_{ad} – change in adhesion performance; $\delta\sigma_{m*}$, $\delta\gamma_{m*}$, δA_{ad*}, $\delta\gamma_{ad*}$ – empirical constants.

Similarly to the article [11], the qualitative criterion of quality for the structural element of nano concrete is given in the form of the ratio:

$$Z_1 = \beta_1 k_1 \cdot k_2 \cdot k_3 + \beta_2 \prod_{i=4}^{7} k_i, \quad (9)$$

where k_1 – the coefficient of the level of reliability of nano concrete; k_2 – the coefficient that characterises the level of strength of the rigid frame; k_3 – the coefficient that characterises the resource of the porous medium; $k_4(D_f)$, $k_5(n_Z)$, $k_6(\sigma_{ve})$, $k_7(K_S)$ – coefficients that characterise the defectiveness D_f, strengthening of the material n_Z, the limit of corrosion fatigue σ_{ve}, taking into account the corrosion resistance of fittings K_S; β_1, β_2 – empirical constants.

Ratios (1), (2), (4), (5), and (8) constitute a new version of the strength criterion for the system nano concrete frame – pore medium. The parameters of the expressions (1), (2), (4), and (5) can be determined based on the experiment, and the parameters of the ratios (8) are estimated based on the computational experiment.

Theory/calculation

The data processing process can be automated using computer programs. The most popular method of viewing information from anywhere is a web page. This way, users can perform calculations and visualise the results in real-time. Bootstrap and ChartJS libraries are used in this work, which is open source and free to use.

These libraries can dynamically configure graphic objects' display parameters and show real-time changes. When the user moves the mouse over the graph points, the digital representation helps the user see the current value. This simplifies data analysis and allows for the extension of the application. In addition, libraries with implemented mathematical algorithms can be used to model various processes, particularly for compressive strength. The data is stored in a database for constant data access and storage of intermediate calculation results. Figure 1 presents a visual view of the information processing results for various nanomaterials [1]. Thus, these results can dynamically change and add new ones as needed. To analyse a specific area, it is possible to increase the scale.

The top three graphs show the difference between the ordinary portland cement paste and three nanomaterials, nanolimestone (NL), nanosilica (NS), and nanoclay (NC). The second row of graphs shows the changes considering the cement-fly ash blended paste (OPCFA).

RESULTS AND DISCUSSION

As a result of data processing determined, the change in the compressive strength σ_* and water and calcium hydroxide content for cement paste after curing parameter when using different mixtures. Comparative graphic characteristics of the parameter change make it possible to estimate the difference in the strengthening of materials each time.

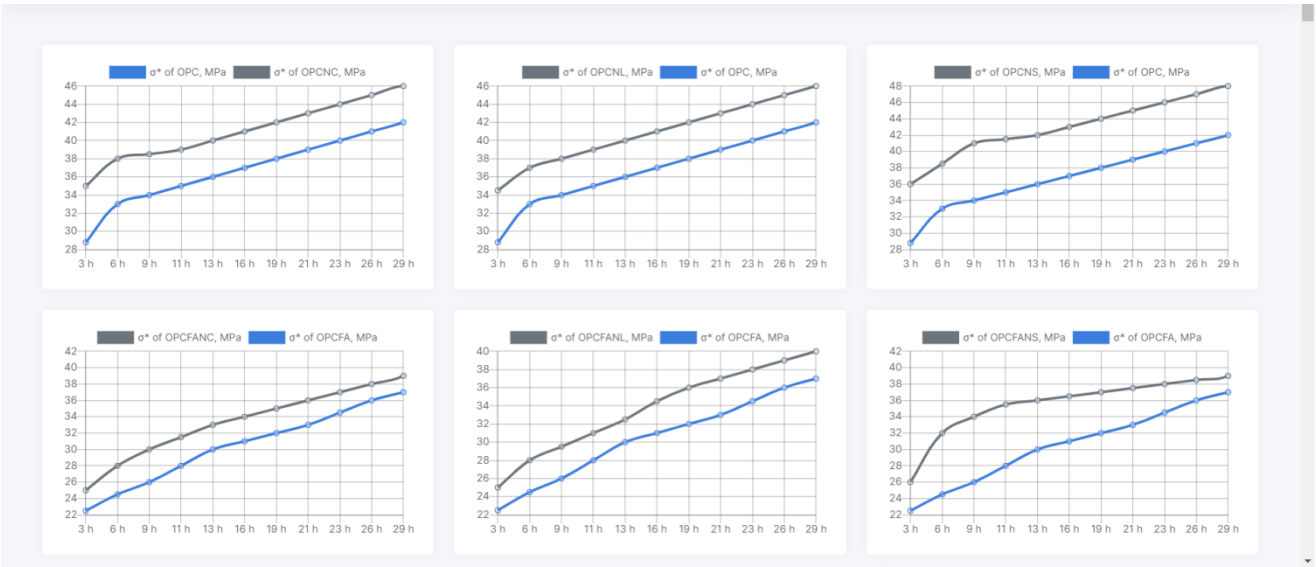

Figure 1 – An example of the results web page

Figure 2 shows the interpolation of water and calcium hydroxide data over time. The change of this parameter from 3 to 29 hours is shown. The upper graph shows the difference in the ordinary portland cement paste (OPC) with the addition of nanomaterials, such as the cement paste with additions of nanolimestone, nanosilica and nanoclay. Chemically bound water increases over time for all nanomaterials, according to the conducted experiment [3].

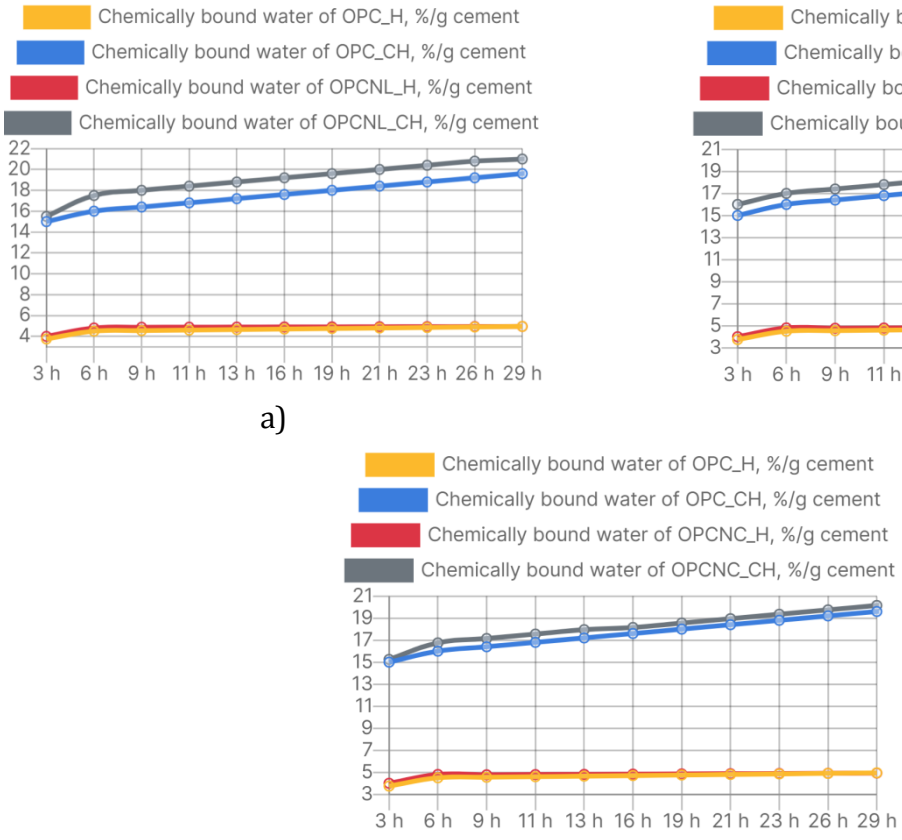

a)

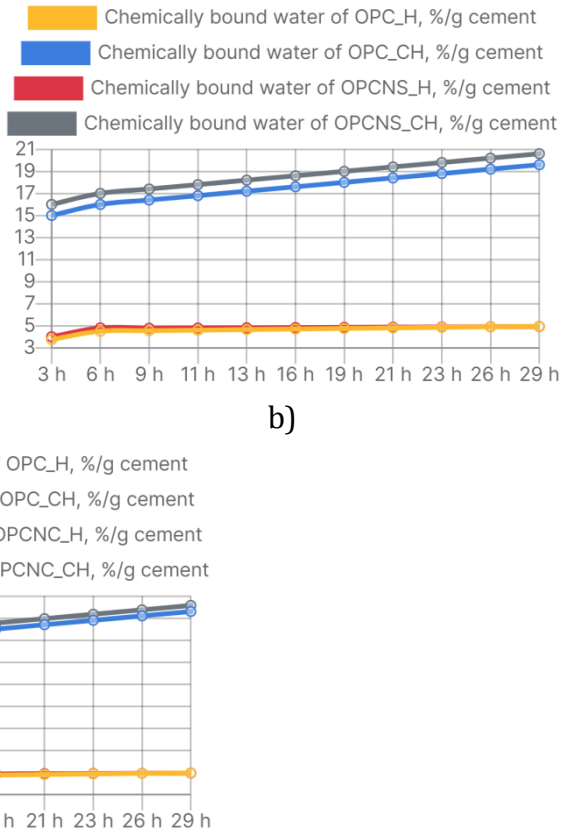

b)

c)

Figure 2 – Interpolation of water and calcium hydroxide content for cement paste after curing

Notes: a) the cement paste with nanolimestone (OPCNL); b) the cement paste with nanosilica (OPCNS); c) the cement paste with nanoclay (OPCNC)

Figure 3 shows the interpolation of these same materials considering the cement-fly ash blended paste (OPCFA). Such a mixture provides cohesion and filling of pores in the cement mixture, which is due to the lower indicators of chemically bound water compared to without the addition of this additive. The lower graph from the upper group of diagrams in this figure takes into account the cement-fly ash blended paste (OPCFA) and the upper ones with the addition of nanoparticles, respectively, in Figure 3a is the cement-fly ash paste with nanolimestone (OPCFANL), in Figure 3b – cement-fly ash paste with nanosilica (OPCFANS), 3c – cement-fly ash paste with nanoclay (OPCFANC). Moreover, the indicators with H shown in the lower group of graphs in Figures 2 and 3 practically do not change over time.

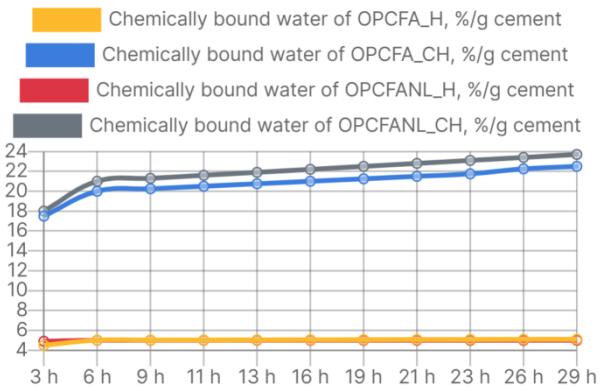

a)

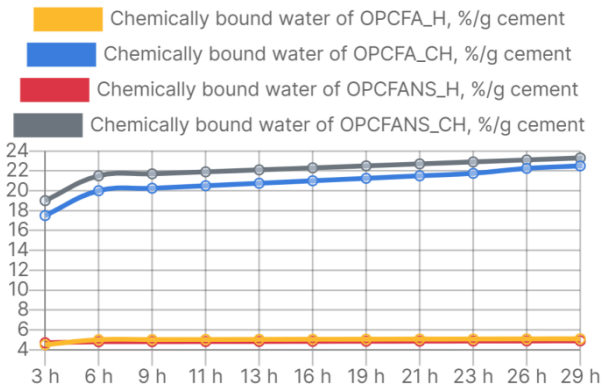

b)

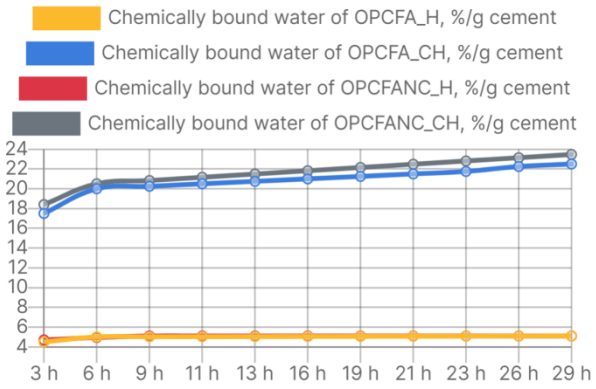

c)

Figure 3 – Interpolation of the content of water and calcium hydroxide for cement-ash paste after curing

Notes: a) cement paste with the addition of nanolimestone (OPCFANL); b) cement paste with the addition of nanosilica (OPCFANS); c) cement paste with the addition of nanoclay (OPCFANC)

Figure 4 shows a linear approximation, which shows the linear nature of changes in this parameter. The percentage deviation from the linear approximation is 17.32% for the ordinary portland cement paste (OPC) is 11.62% with NS, 10.28% – NL, and 7.6% – NC. Among all nanoparticles, the compressive strength increases linearly in a cement mixture with nanoclay. The most significant difference is observed in the first points due to the use of a linear approximation.

Figure 5 shows the overlay of the linear approximation on changes in the compressive strength parameter. On these graphs, compared to the cement-ash mixture and nanoparticles, the percentage difference between the linearly approximated straight line and the compressive strength change graph: cement-fly ash paste (OPCFA), 41.4% – cement-fly ash paste with nanolimestone (OPCFANL) (Fig. 5a), 17.71% – cement-fly ash paste with nanosilica (OPCFANS) (Fig. 5b), 20.75% – cement-fly ash paste with nanoclay (OPCFANC) (Fig. 5c). It can be assumed that the square root function is more suitable for such materials.

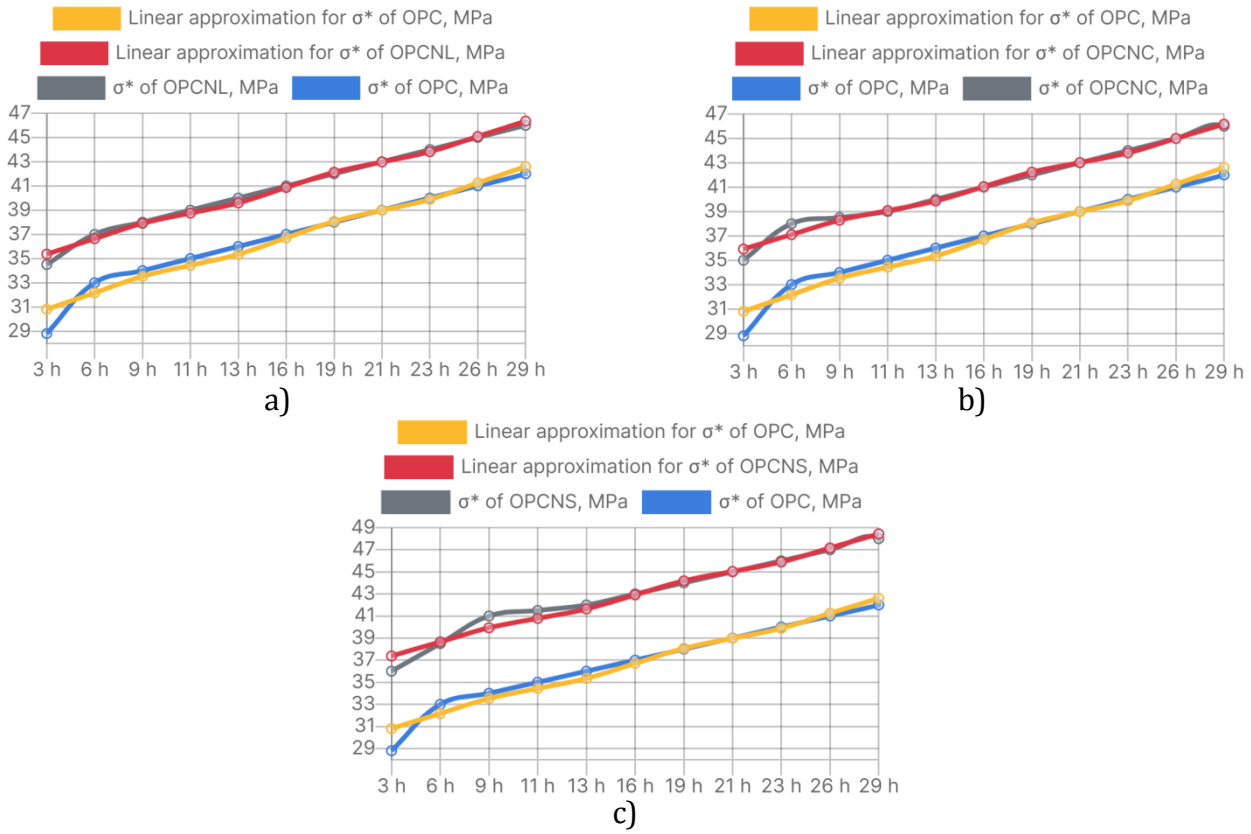

Figure 4 – Approximation of the compressive strength σ_* for cement paste with: a) cement paste with the addition of nanolimestone (OPCNL); b) cement paste with the addition of nanosilica (OPCFAS); c) cement paste with the addition of nanoclay (OPCNC)

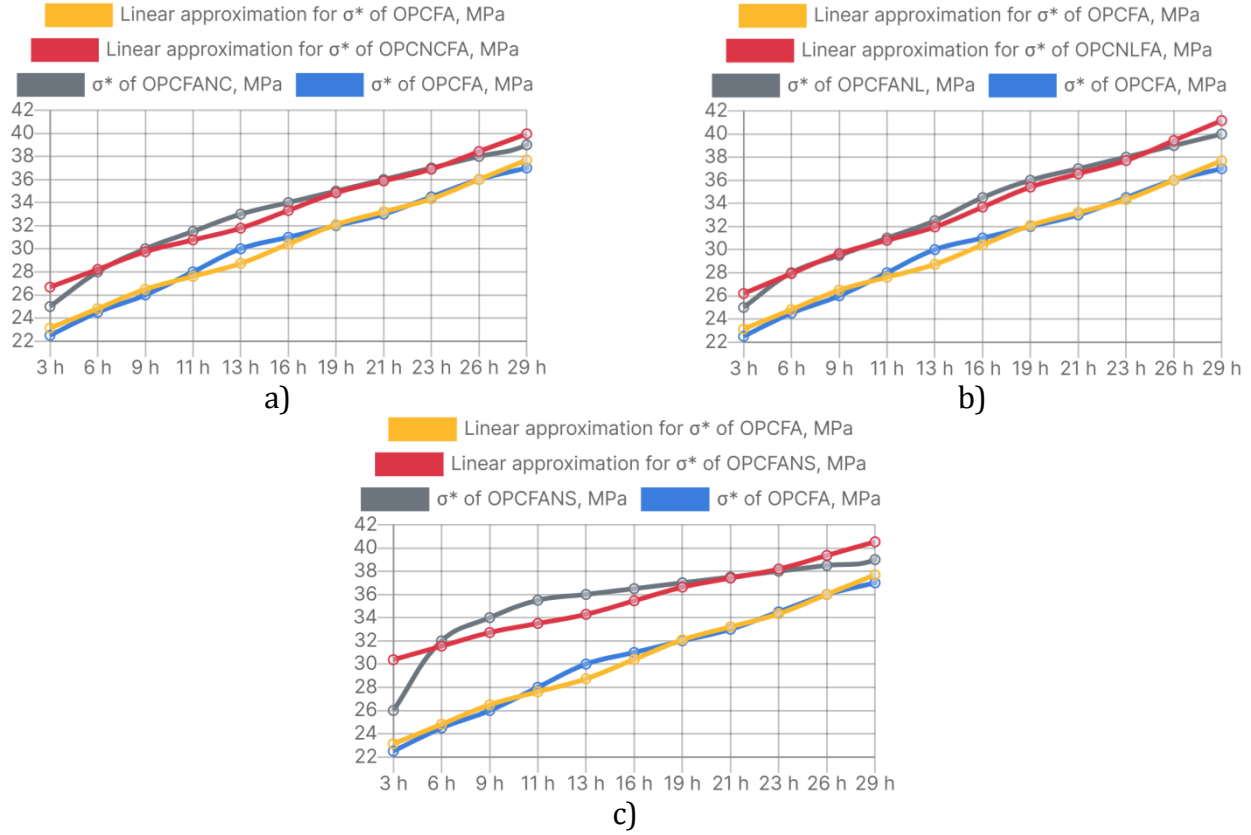

Figure 5 – Approximation of the compressive strength σ_* for cement-fly ash paste (OPCFA)

Notes: a) cement-fly ash paste with nanolimestone (OPCFANL); b) cement-fly ash paste with nanosilica (OPCFANS); c) cement-fly ash paste with nanoclay (OPCFANC)

Table 1 shows the percentage difference between the compressive strength of ordinary cement paste (OPC) and with the addition of nanomaterials of nano limestone (OPCNL), nanosilica (OPCNS) and nanoclay (OPCNC) over time-based on Figure 2a, 2b and 2c.

Table 1 – The percentage difference between the compressive strength σ_* of the ordinary cement mixture (OPC) and with the addition of the nanomaterials of nanolimestone (OPCNL), nanosilica (OPCNS), nanoclay (OPCNC) and cement-fly ash paste (OPCFA) and with the addition of the nanomaterials of nano-limestone (OPCFANL), nanosilica (OPCFANS), and nanoclay (OPCFANC) over time

Time, h	σ_* of OPCNL, %	σ_* of OPCNS, %	σ_* of OPCNC, %	σ_* of OPCFANL, %	σ_* of OPCFANS, %	σ_* of OPCFANC, %
3	13.51	13.95	9.75	10.14	15.07	8.82
6	19,79	20	17,71	10	13,46	10
9	13,15	13,63	9,52	11,11	13,51	8,57
11	12,82	13,33	9,3	10,81	12	8,33
13	12,12	14,28	13,15	12,5	23,43	12,5
16	12,5	13,04	9,09	9,21	9,21	6,76
19	13,23	17,07	11,7	11,86	23,52	13,33
21	12,19	12,76	8,88	7,69	6,49	5,26
23	14,28	15,66	10,25	9,68	21,13	11,11
26	13,89	14,28	10	7,69	16,67	9,09
29	11,9	12,5	8,69	7,5	5,12	5,12
Mean	13,51	16,975	9,875	10,07	18,05	9,41

As shown in Table 1, with the addition of nanoparticles, all materials have higher destructive load indicators and become stronger. The most significant average deviation from the usual mixture in strength with the addition of nanosilica to the cement mixture (OPCNS) and less with the addition of nanoclay (OPCNC). On average, when added to a conventional cement mixture, the addition of nanoparticles equals 13.45%.

With the addition of nanosilica (OPCFANS) to the cement-ash mixture, such a mixture becomes the strongest. Compared to the cement mixture with nanosilica, the same combination is still worse in terms of results since the values obtained for compressive strength in Figure 2 have higher values of compressive strength compared to those with the cement-ash mixture in Figure 3.

By selecting approximation, it is possible to summarise the characteristics of the change of these parameters. This mathematical analysis allows you to work out and analyse the results. Theoretical results can be simulated programmatically using the developed web page. Different pastes can be programmatically affected and compare theoretical results in this case.

Table 1 shows the percentage difference for different pastes with additives in each period. It can conclude the strength based on the compressive strength indicators. For cement and cement-ash pastes and with nanosilica, nanoclay and nanolimestone nanoparticles, data analysis is performed using linear interpolation and approximation methods to determine the nature of the compressive strength parameter.

Since the linear approximation is possible for deviation values that are not significant, it can be assumed that the strengthening coefficient increases linearly for cement paste and the behaviour of the square root function (branch of the parabola) for cement-ash pastes for a period from 3 hours to 29 hours. However, if it is considered that the beginning is from 1 hour, then in the first hours, this parameter increases the most and, in general, resembles the branch of a parabola.

Another parameter of strength can be considered the water and calcium hydroxide content after curing.

The paper also mathematically shows the influence of the destructive load parameter on changes in the quality of nano concrete, which can be used to assess strength and corrosion processes.

CONCLUSIONS

1. A new version of the nano concrete strength criterion is proposed, taking into account the en-

ergy characteristics of the interphase layers between the solid framework and the micropore medium, which characterise the connections (adhesion) of the two media.

2. The relationship between surface physics and fracture mechanics is the basis of the methodology for assessing the quality of nano concrete and can be used to determine the resource of the material and the strengthening parameter, taking into account the criteria of strength, corrosion processes and metrological support.

3. Based on the obtained results, the strength, reliability, strengthening parameter and residual resource of nano concrete can be evaluated, taking into account the porous medium.

4. With the help of software modelling using mathematical methods, it is possible to improve the structure, manipulate the number of nanomaterials, and determine the characteristics of nano concrete.

REFERENCES

1. Popova, N., Kataiev, A., Skrynkovskyy, R., & Nevertii, A. (2019). Development of trust marketing in the digital society. *Economic Annals-XXI, 176*(3–4), 13–25. doi: 10.21003/ea.v176-02
2. Popova, N., Kataiev, A., Nevertii, A., Kryvoruchko, O., & Skrynkovskyi, R. (2021). Marketing Aspects of Innovative Development of Business Organizations in the Sphere of Production, Trade, Transport, and Logistics in VUCA Conditions. *Studies of Applied Economics, 38*(4). doi: 10.25115/eea.v38i4.3962
3. Wang, X. (n.d.). *Effects of nanoparticles on the properties of cement-based materials*. doi: 10.31274/etd-180810-5865
4. Psakhie, S. G., Dimaki, A. V., Shilko, E. V., & Astafurov, S. V. (2015). A coupled discrete element-finite difference approach for modeling mechanical response of fluid-saturated porous materials. *International Journal for Numerical Methods in Engineering, 106*(8), 623–643. doi: 10.1002/nme.5134
5. Konovalenko, Ig. S., Shilko, E. V., & Konovalenko, Iv. S. (2020). The Numerical study of the influence of a two-scale pore structure on the dynamic strength of water-saturated concrete. *PNRPU Mechanics Bulletin, 2*, 37–51. doi: 10.15593/perm.mech/2020.2.04
6. Garavand, A., Stefanov, Y. P., Rebetsky, Y. L., Bakeev, R. A., & Myasnikov, A. V. (2020). Numerical modeling of plastic deformation and failure around a wellbore in compaction and dilation modes. *International Journal for Numerical and Analytical Methods in Geomechanics, 44*(6), 823–850. doi: 10.1002/nag.3041
7. Biot, M. A. (1941). General Theory of Three-Dimensional Consolidation. *Journal of Applied Physics, 12*(2), 155–164. doi: 10.1063/1.1712886
8. Alejano, L. R., & Bobet, A. (2012). Drucker–Prager Criterion. *Rock Mechanics and Rock Engineering, 45*(6), 995–999. doi: 10.1007/s00603-012-0278-2
9. Tercaghi, K. (2008). *Theoretical Soil Mechanics*. New York: Wiley.
10. Yuzevych, V. M., Dzhala, R. M., & Koman, B. P. (2018). Analysis of Metal Corrosion under Conditions of Mechanical Impacts and Aggressive Environments. *Metallofizika i Noveishie Tekhnologii, 39*(12), 1655–1667. doi: 10.15407/mfint.39.12.1655
11. Yuzevych, L., Yankovska, L., Sopilnyk, L., Yuzevych, V., Skrynkovskyy, R., Koman, B., Yasinska-Damri, L., Heorhiadi, N., Dzhala, R., & Yasinskyi, M. (2019). Improvement of the toolset for diagnosing underground pipelines of oil and gas enterprises considering changes in internal working pressure. *Eastern-European Journal of Enterprise Technologies, 6*(5), 23–29. doi: 10.15587/1729-4061.2019.184247
12. Yuzevych, V., Pavlenchyk, N., Zaiats, O., Heorhiadi, N., & Lakiza, V. (2020). Qualimetric Analysis of Pipelines with Corrosion Surfaces in the Monitoring System of Oil and Gas Enterprises.

International Journal of Recent Technology and Engineering, 9(1), 1145–1150. doi: 10.35940/ijrte.a1341.059120

13. Lozovan, V., Skrynkovskyy, R., Yuzevych, V., Yasinskyi, M., & Pawlowski, G. (2019). Forming the toolset for development of a system to control quality of operation of underground pipelines by oil and gas enterprises with the use of neural networks. *Eastern-European Journal of Enterprise Technologies, 2*(5), 41–48. doi: 10.15587/1729-4061.2019.161484
14. Yuzevych, V., Skrynkovskyy, R., & Koman, B. (2018). Intelligent Analysis of Data Systems for Defects in Underground Gas Pipeline. *2018 IEEE Second International Conference on Data Stream Mining Processing*. doi: 10.1109/dsmp.2018.8478560
15. Yuzevych, L., Skrynkovskyy, R., & Koman, B. (2017). Development of Information Support of Quality Management of Underground Pipelines. *EUREKA: Physics and Engineering, 4*, 49–60. doi: 10.21303/2461-4262.2017.00392